Volume shrinking in Micro-Fluidic Self-Assembly

Jan Lienemann, Andreas Greiner and Jan G. Korvink
IMTEK – Institute for Microsystem Technology, Albert Ludwig University
George Köhler Allee 103, D-79 110 Freiburg, Germany
Tel. +49 761 203 7380, Fax. +49 761 203 7382
lieneman@imtek.de

Abstract

Self assembly in the fluidic phase is a technique excellently suited for the parallel assembly of millions of micro-parts, as it is necessary for pixel displays.

In this work, we investigate the effect of volume shrinking during the hardening of the glue and discuss the implications for the design of the assembled micro-parts.

We simulate the response of the micro-part position to an inhomogeneous polymerization process and provide guidelines to the material choice for the glue.

1. Introduction

For the production of pixel displays, it is often desirable to combine numerous materials and processes. Incompatibilies often impede a monolithic integration. Hybrid integration processes allow for processing each component in a separate step and assembling them later on a common substrate.

Micro-fluidic self-assembly is a promising candidate for this need. The fluidic system consists of a binding site with a hydrophobic self-assembled monolayer (SAM), the micro-part featuring also a hydrophobic face and the glue monomer, which furthermore functions as lubricant (see Fig. 1).

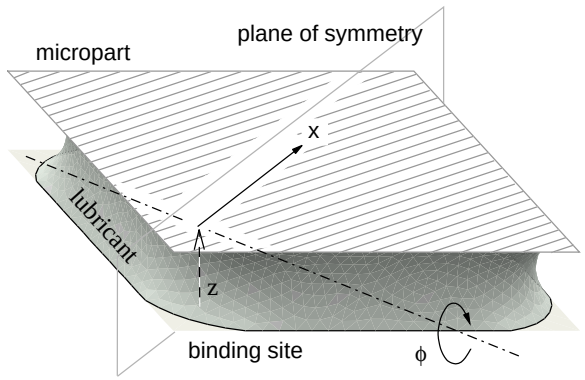

Figure 1. Geometry of the assembled micro-part. The part displacements are measured in a global coordinate frame with origin on the binding site. The system is symmetric w. r. t. the ϕ-axis.

First, the glue (G) is supplied to the binding site (B), covering most of it due to surface tension ($\gamma_{GB} < 1\,\mathrm{mJ/m^2}$). For the assembly, the entire system is immersed in water (W, $\gamma_{WB} = 52\,\mathrm{mJ/m^2}$, $\gamma_{WG} = 46\,\mathrm{mJ/m^2}$). Then the micro-parts are poured onto the substrate. As soon as their hydrophobic face touches the lubricant, they are pulled to the binding site and aligned by capillary forces. Xiong, et al. [1] used triethyleneglycol dimethacrylate (TEGDMA) as glue (Fig. 2).

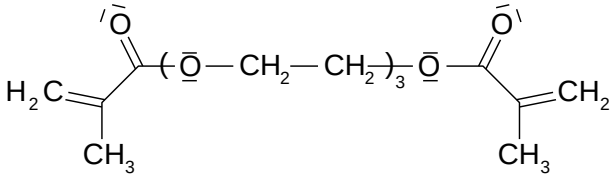

Figure 2. Triethyleneglycol dimethacrylate (TEGDMA).

While the exact angular position of simple light emitting diodes is rather insignificant, it becomes crucial when mirrors or directed light beams like LASERs are involved.

In fluidic self-assembly processes, the parallel alignment of the micro-part is ensured by the surface tension of the glue, if the parameters are correctly chosen such that symmetry is enforced [2].

This ideal case is given as long as the glue is liquid and the polymerization process has not started yet. As the volume of the glue decreases during the reaction, a homogeneous hardening is required to fix this aligned state.

The nature of the polymerization requires radical starter molecules. Breaking the starter molecule into two parts, two radicals form. These radicals break a double bond in the monomer and initiate the linking of the polymer chain.

The dissociation of the starting molecule is achieved by heating and therefore at temperatures above 80 °C thermal break-up occurs. But in the presence of metal, a catalytic reaction at lower temperatures is possible.

Since the SAM is assembled on a gold film with different other metals as adhesive layers below, an exposure of metal to the glue is possible, resulting in an early start of the polymerization. This is quite probable at the corners of the pads, if the underlying layers are not protected. We therefore assume that the polymerization starts at a bind-

ing site corner and continues spherically. Since the height of the glue (200 µm) is small compared to its lateral extent (side length 1 mm), we approximate the sphere by a cylinder.

2. Simulation

The simulation procedure consists of three parts:

a) Find the equilibrium state of the system
b) Increase the radius of the hardened glue cylinder
c) Insert the elastic energy of the glue into the energy calculation

To calculate the shape of the liquid meniscus and find the equilibrium, we used the *surface evolver* software by K. A. Brakke [3]. For the simulation of solid elastic properties we used *ANSYS* [4]. The elasticity parameters of the TEGDMA glue (Young's Modulus $Y = 2\,\mathrm{GPa}$, Poisson's number $\nu = 0.4$) are estimated from literature data [5]. As a result we expressed the elastic behaviour as a simple spring model. To tackle the various states of glue hardening, we calculated a series of spring constants for different glue cylinder radii and represented them as a polynomial fit (see Fig. 4). This results in the following simulation scheme:

1. Find the equilibrium shape of the completely liquid meniscus in the *surface evolver*
2. Transfer the geometry to *ANSYS* and perform an elastostatic analysis for different radii
3. Find a polynomial fit and implement it in the surface evolver
4. Main simulation loop (steps a–c above)

2.1. Equilibrium meniscus shape

The shape of the meniscus is calculated by the surface evolver. The z position of the micro-part is adjusted by an iterative Newton minimization of the total energy. The first and second derivatives are calculated with finite differences of the total energy and Lagrange multipliers. On failure of a Newton step, a small steepest descent step is performed and the Newton iteration is repeated.

2.2. Transfer to *ANSYS*

For transferring the meniscus shape to *ANSYS*, the vertex coordinates and the mapping of area elements to vertices are extracted from the *surface evolver* to an APDL (ANSYS Parametric Design Language) command file.

Since our model used in the *surface evolver* consists only of the lateral faces of the glue (the top and bottom areas are calculated by line integrals [6]), we add the top and bottom areas manually. Therefore, we express the position of the top vertices in polar coordinates. After sorting them by angle, we create triangles for each two subsequent points and the midpoint of the respective area.

After that, we cut out different glue radii (Fig. 3), make the top area rigid, fix the bottom area and perform an elastostatic analysis for compression in z direction, shear in x direction and a moment load around the dashed axis in Fig. 1.

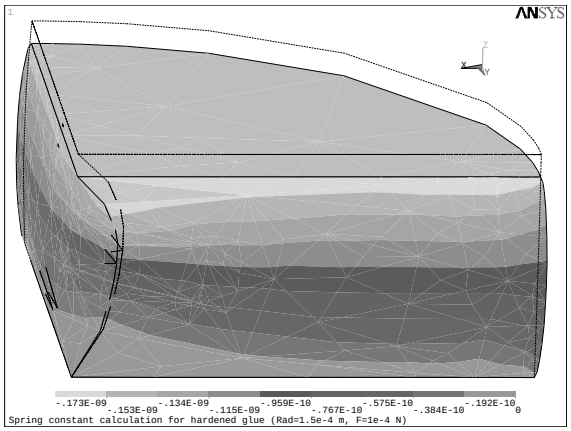

Figure 3. *ANSYS* simulation of hardened glue. The empty black outline shows the undeformed shape, the contours show the z displacement.

2.3. Implementation of elastic effects

For the spring constants K a polynomial fit of order 4 is found. Our goal was to be as exact as possible for the moment load at low radii, because the largest deflection is expected at the beginning of the hardening process. As shown in Fig. 4, the errors introduced by this fit are negligible.

Since we consider linear elastostatics, we can separate the elastic energy for the three degrees of freedom x (lateral deflection), z (perpendicular to the micropart) and ϕ (bending) and superpose in the following calculation.

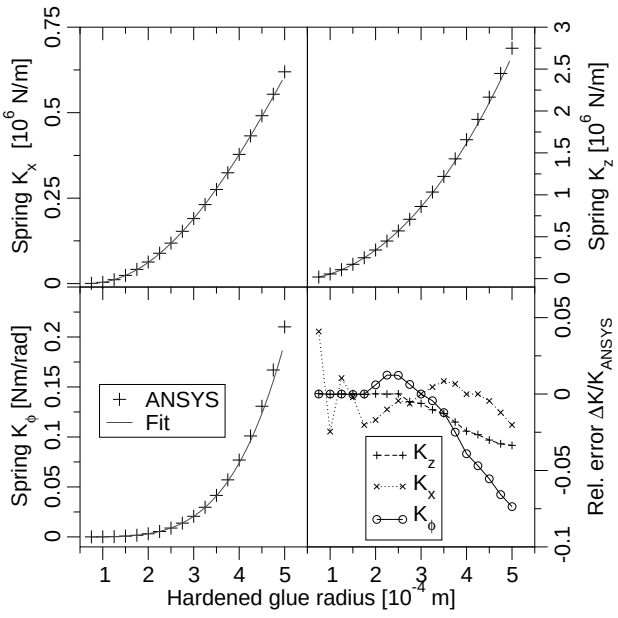

Figure 4. Polynomial fits for spring constants.

The z direction spring energy for a given glue radius r can then be written as

$$\begin{aligned} E(r,z) &= \frac{1}{2}\int_0^r k(\xi)\,[z - z_0(\xi)]^2\,\mathrm{d}\xi \\ &= \frac{1}{2}z^2\int_0^r k(\xi)\,\mathrm{d}\xi - z\int_0^r k(\xi)z_0(\xi)\,\mathrm{d}\xi + \\ &\quad + \frac{1}{2}\int_0^r k(\xi)z_0^2(\xi)\,\mathrm{d}\xi \qquad (1) \\ &= c_2 z^2 + c_1 z + c_0 \qquad (2) \end{aligned}$$

where $k(r) = \mathrm{d}K_z/\mathrm{d}r$ and $z_0(r)$ is the z deflection of the micropart when the glue radius was r. For x and ϕ the same consideration applies.

For a finite integration step, we get

$$c_0(r+\Delta r) \approx c_0(r) + \frac{1}{2}z_0^2(r)\,[K_z(r+\Delta r) - K_z(r)] \qquad (3)$$

$$c_1(r+\Delta r) \approx c_1(r) - z_0(r)\,[K_z(r+\Delta r) - K_z(r)] \qquad (4)$$

$$c_2(r+\Delta r) = \frac{1}{2}K_z(r+\Delta r) \qquad (5)$$

The same applies for the x and ϕ deflections.

The liquid glue is then constrained such that the monomer-polymer interface lies on a cylinder and contributes no surface energy (Fig. 5). Since the algorithm may increase the area of the cylinder without cost, we always find an offset angle at the initial simulation step, and occasionally also at the second simulation step if the maximum number of iterations in the first simulation step is reached. This initial angle is therefore subtracted from the result, and only the difference is quoted. Because of the very low elastic constants of the glue in this early step, the error in the result is negligible.

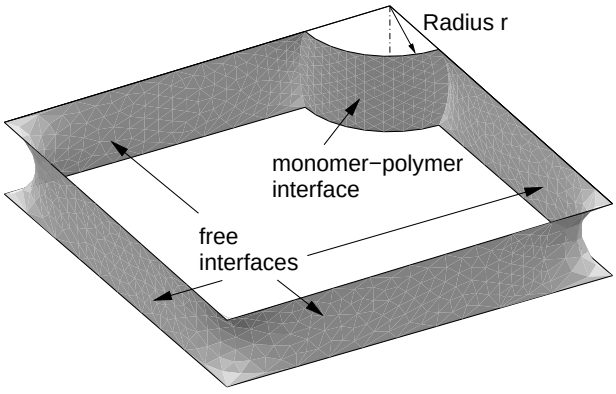

Figure 5. The monomer-polymer interface is constrained to a cylindrical shape.

2.4. Volume shrink

During the polymerization of the glue, the volume may shrink up to $\beta = 20\%$ [7]. This means that an increase $\mathrm{d}V_G$ in the polymer volume reduces the monomer volume by $\mathrm{d}V_M = -\mathrm{d}V_G/0.8$. So the change for the monomer volume for a glue radius change from $r_1 = r$ to $r_2 = r + \Delta r$ may be written as

$$\Delta V_M = -\frac{1}{1-\beta}\int_{r_1}^{r_2}\int_0^{\frac{\pi}{2}} z \cdot r\,\mathrm{d}\theta\,\mathrm{d}r. \qquad (6)$$

Deploying the symmetry of the setup, we can write that

$$z = z_c - r \cdot \tan\phi \cdot \sin(\theta + \frac{\pi}{4}) \qquad (7)$$

where z_c is the z position of the chip corner. This yields a volume change of

$$\Delta V_M = -\frac{1}{1-\beta}\left[\frac{\pi}{4}\left(r_2^2 - r_1^2\right)z_c - \frac{\sqrt{2}}{3}\left(r_2^3 - r_1^3\right)\tan\phi\right] \qquad (8)$$

2.5. Integration step

One integration step consists of updating the spring constants with (3)–(5), the volume with (8) and adjusting the constraints to reflect the advanced glue. Vertex averaging and equiangulation ensure a uniform grid. We assume that the glue hardening happens on a much larger timescale than fluidic relaxation, i. e. the fluid shape follows adiabatically. Thus the energy with respect to x, z and ϕ is always minimal.

3. Results

For different volume shrink values β, we performed the simulation for several Young's moduli Y by scaling the spring constants appropriately. The glue radius increase per simulation step is $10^{-5}\,\mathrm{m}$.

We observed a tilting angle depending on both parameters. For high values of β, we noticed a relaxation of the angle at later integration steps (Fig. 7). The reason is the decrease in interface area to water and therefore a smaller surface tension force.

The results are printed in Table 1. The first line denotes the difference between the maximum angle and the initial angle. When the relaxation effect is greater than the accuracy of the table values, the relaxed angle at integration step 30 is printed in the second line.

High β values are unlikely to occur in polymerization; for drying processes, however, the evaporation of the solvent may impose a larger volume shrink on the glue.

4. Conclusion

We simulated the angular displacement of a micropart in micro-fluidic self-assembly due to inhomogeneous hardening of the glue at a given corner. The final angle depends on both the relative volume shrink of the glue and Young's modulus of the hardened glue. For an extreme example, a displacement of more than 5° was observed. With high volume shrink, the angle might relax later. For a smaller meniscus height, smaller angles can be expected due to higher spring constants.

Table 1. Tilting angle (in degrees) of the micro-part as a function of Young's modulus Y and shrinking ratio β. Values in parenthesis were noisy.

β \ Y/MPa	10	20	40	80	150	300	750	2000
0.2	0.0857	0.0657	(0.0372)	(0.0411)	0.0171	0.0114	0.00728	0.00308
0.4	0.266	0.185	0.127	0.0835	0.0576	0.0296	0.0171	0.00568
0.6	0.655	0.462	0.336	0.232	0.157	0.106	0.0648	0.0277
0.7	0.991	0.711 0.710	0.504	0.356	0.240	0.168	0.0899 0.0898	0.0430
0.8	1.63 1.62	1.20 1.19	0.862 0.856	0.617 0.614	0.435 0.433	0.305 0.304	0.167 0.166	0.0818 0.0816
0.9	3.49 3.33	2.62 2.54	1.95 1.90	1.41 1.39	1.00 0.99	0.678 0.670	0.366 0.362	0.160 0.159
0.95	5.36 5.35	4.70 4.59	3.49 3.30	2.49 2.38	1.78 1.72	1.20 1.17	0.666 0.651	0.323 0.317

For the material system chosen by Xiong, et al., only a negligible angular displacement was found, since Young's modulus is high and the volume shrink is low enough. With a careful choice of the glue material and by introduction of an exposed metal pad at one corner, these results could also be used as a method to produce micro-parts with a defined tilting angle.

5. Acknowledgments

The authors would like to thank Karl F. Böhringer of the University of Washington for various discussions and K. A. Brakke for making available the *surface evolver* program and for providing extensive documentation.

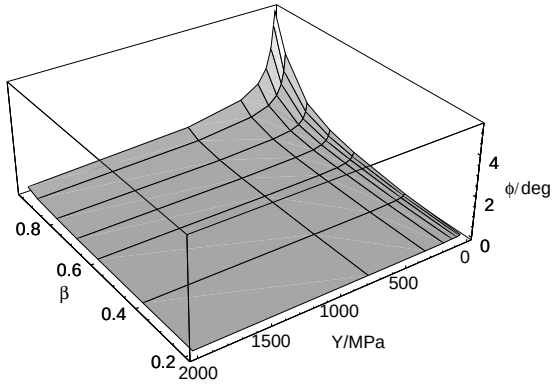

Figure 6. 3D plot of the results in Table 1.

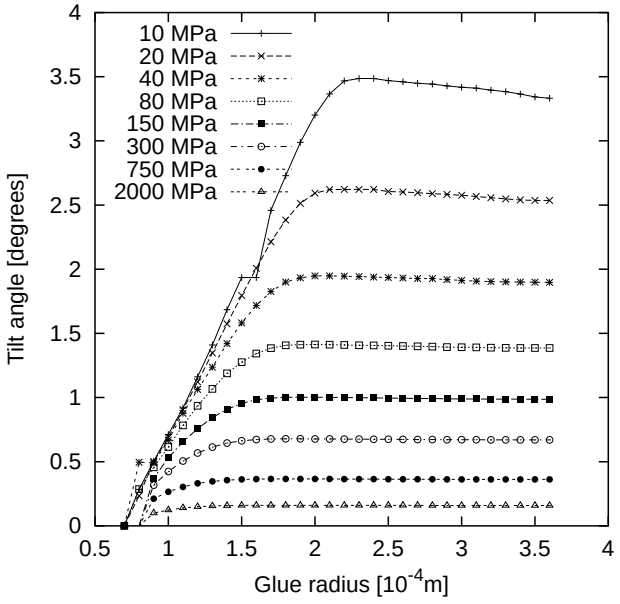

Figure 7. Micro-part tilting angle versus hardened glue radius for $\beta = 0.9$. The relaxation of the tilting angle is clearly visible. Each curve corresponds to a specific value of Young's modulus.

6. References

[1] X. Xiong, Y. Hanein, W. Wang, D. T. Schwartz and K. F. Böhringer, "Controlled part-to-substrate micro-assembly via electrochemical modulation of surface energy", *Proc. Int. Conf. on Solid-State Sensors and Actuators*, Munich, Germany, 2001.

[2] A. Greiner, J. Lienemann, J. G. Korvink, X. Xiong, Y. Hanein and K. F. Böhringer, "Capillary Forces in Micro-Fluidic Self-Assembly", *Tech. Proc. MSM*, San Juan, Puerto Rico, USA, 2002.

[3] K. A. Brakke, "Surface Evolver Manual", 1999, http://www.susqu.edu/facstaff/b/brakke/

[4] ANSYS, Inc., "ANSYS User's Manual Revision 5.7", Canonsburg, USA, 2000

[5] Sartomer Company, "Coating concepts", Vol. IV, 2001, http://www.sartomer.com/wpapers\3043.pdf

[6] J. Lienemann, A. Greiner and J. G. Korvink, "Surface Tension defects in Micro-Fluidic Self-Alignment", *accepted for publication in Proc. DTIP 2002*, Cannes Mandelieu, France, 2002

[7] K. F. Böhringer, *private communication*, Feb. 2002